

# Improved Angular Resolution with GQI2: a new Diffusion Imaging Q-Space Cartesian Lattice Reconstruction Method

Ian Nimmo-Smith<sup>1</sup>, Fang-Chen Frank Yeh<sup>2</sup>, and Eleftherios Garyfallidis<sup>3</sup>

<sup>1</sup>MRC Cognition and Brain Sciences Unit, Cambridge, Cambridgeshire, United Kingdom, <sup>2</sup>Biomedical Engineering, Carnegie Mellon University, Pittsburgh, PA, United States, <sup>3</sup>University of Cambridge, Cambridge, Cambridgeshire, United Kingdom

**TARGET AUDIENCE:** Practitioners and researchers who collect and analyze data from Cartesian Lattice Q-Space acquisition schemes such as those used in diffusion spectrum imaging (DSI).

**PURPOSE:** To obtain improved angular resolution in orientation distribution functions (ODF). Orientation Distribution Functions (ODFs) summarise the evidence for any particular direction being present in the fiber composition of a voxel, with the peaks of the ODF being used to generate tractography streamlines. Low angles between different fiber tracts within a voxel are one of the principal limiting factors to using diffusion weighted MR imaging (dMRI) to exploring white matter tractography in the brain accurately.

**THEORY:** Diffusion Spectrum Imaging (DSI) [1] exploits the theoretical direct route from dMRI acquired on a Cartesian grid in q-space to the local diffusion propagator  $P$  via a Fourier transform of the modulus of the signal  $S$ , followed by a radial projection to give the DSI-ODF  $\psi_{DSI}(u) = \int P(ru) r^2 dr$  where  $u$  is a point of the ODF sphere and  $r$  is the spin displacement vector. Generalised Q-Sampling Imaging (GQI) [2] introduced GQI-ODF, an unweighted truncated radial projection of the Fourier transform of the signal, showed that GQI-ODF could be calculated more directly as a sinc-transform of the raw signal, with the projection cutoff  $\lambda$  acting as a smoothing parameter  $\psi_{GQI}(u) = \lambda \int S(q) \text{sinc}(2\pi \lambda q \cdot u) dq$  where  $q$  is the q-space wave vector. Yeh et. al [2] showed that GQI has a better angular resolution of fiber crossings than DSI. We introduce GQI2, a new signal transform by reintroducing the radial distance weighting in the radial projection of the diffusion propagator  $\psi_{GQI2}(u) = \lambda^3 \int S(q) H(2\pi \lambda q \cdot u) dq$  where  $H(x \neq 0) = 2\cos(x)/x^2 + (x^2 - 2)\sin(x)/x^3$  and  $H(0) = 1/3$ . Because of the direct analytical formulation of  $\psi_{GQI}$  and  $\psi_{GQI2}$  it is not necessary to create the volumetric grid with the signal values and thus GQI and GQI2 are more efficient in terms of computer memory and CPU. We show that GQI2 has significantly improved ability to resolve fiber directions over the established techniques of DSI and GQI over a range of signal-to-noise ratios. The non-parametric nature of the algorithms described here allows for the identification of multiple fiber crossings, by contrast with DTI which fails in this regard. GQI2 can be expressed algorithmically as a direct linear transform of the raw signal [3].

**METHODS:** The three methods DSI, GQI and GQI2 were compared using simulations and healthy human in vivo data. Simulations with stick-and-ball models of fibers [4] were generated with added Rician noise. The human data is available online at [cmrk.org](http://cmrk.org) from the Diffusion Group at École Polytechnique Fédérale de Lausanne (EPFL), Switzerland. (3T scanner with a 32 channels head coil; field of view was 210x210 mm<sup>2</sup>, matrix 96x96, slice thickness 3 mm; 44 slices, voxel resolution 2.2x2.2x3mm<sup>3</sup>; a 258-point half grid acquisition scheme with a maximum b-value of 8011 s mm<sup>2</sup> was used; the total acquisition time was 34 min with TR=8200 ms and TE=165 ms.)

**RESULTS:** In Fig. 1 we see an experiment on two crossing fibers using the three different reconstruction methods DSI, GQI and GQI2. These are based on simulations of 2-fiber crossings from 0° to 90° with diffusivity value of 1.5x10<sup>-3</sup> mm<sup>2</sup>/sec and 257 b-values with maximum b-value 11,000. All methods perform accurately beyond 50° so this figure only presents results for the lower angles. We can see that GQI2 performed better than the other methods overall being able to resolve the two directions when the angle was about 35°. In order to compare the angular precisions of the ODFs we defined a new similarity metric called Angular Similarity (AS) which computes the cosine distance of the best match between the set of measured fiber orientations and the known set of simulated fibers. This metric will be used to compare 2-fibre and 3-fibre crossings. AS is 0 when there is no match i.e. angular distance is 0, 1 when one fiber is matched (0°), 2 when two fiber are matched and 3 when three fibres are matched. Here DSI has radial sampling 2.1 – 6, and hanning filter width 36; GQI: has  $\lambda = 1.2$ ; and GQI2 has  $\lambda = 3$ . In Fig. 2, based on approximately 200 simulations per angle, we see that GQI2 performs better than DSI which in turn is better than GQI at resolving three fibers crossing at equally inclined directions. The same pattern holds when the noise level is increased and also when a 2 fiber crossing is simulated. Fig. 3 compares DSI (radial sampling 2.1-6; hanning filter width 36), GQI ( $\lambda = 1.2$ ) and GQI2 ( $\lambda = 3$ ) on the human data using a reconstruction sphere with 642 vertices and 1280 faces. The results are overlaid on an FA slice. Again GQI2 resolves directions more sharply than GQI and is broadly similar to DSI. Differences between GQI2 and DSI will be more fully explored in a future report.

**DISCUSSION and CONCLUSION:** GQI2 has superior performance over DSI and GQI concerning angular resolution. It also generates smoother ODFs and it is faster to calculate than DSI. Any resulting tractography based on GQI2 will more accurately reflect complexity of underlying fiber structure with multiple crossings than GQI or DSI. A python implementation of GQI2 is available at [dipy.org](http://dipy.org).

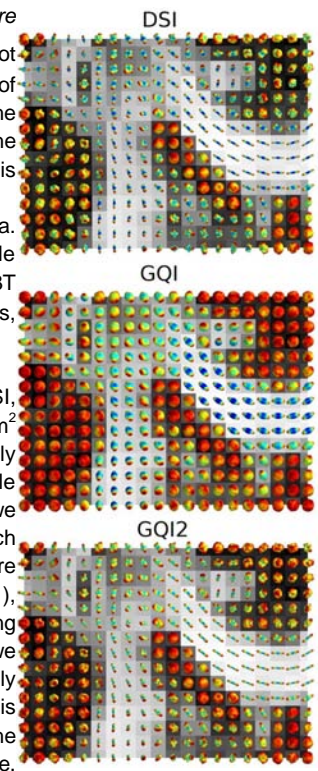


Figure 3

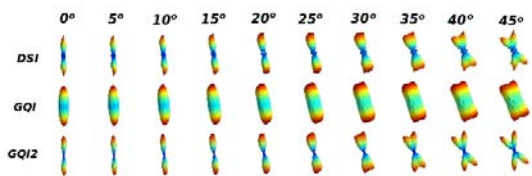


Figure 1

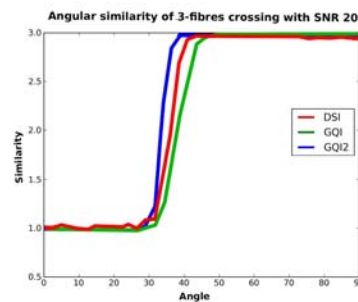


Figure 2

**REFERENCES:** [1] Wedeen et. al (2005) MRM, [2] Yeh et. al 2010 IEEE TMI, [3] Garyfallidis, (2012) PhD thesis, [4] Behrens et. al (2007) Neuroimage.